Original Paper

American Society for Neurochemistry

ASN Neuro
Volume 11: 1–17

DOI: 10.1177/1759091419892090
journals.sagepub.com/home/asn
SAGE

Neuronal Conditional Knockout of Collapsin Response Mediator Protein 2 Ameliorates Disease Severity in a Mouse Model of Multiple Sclerosis

Aubin Moutal[1], Sergey Kalinin[2], Kathy Kowal[2], Natalia Marangoni[2], Jeffrey Dupree[3], Shao Xia Lin[2], Kinga Lis[2], Lucia Lisi[4], Kenneth Hensley[5], Rajesh Khanna[1] and Douglas L. Feinstein[2,6]

Abstract

We previously showed that treatment with lanthionine ketimine ethyl ester (LKE) reduced disease severity and axonal damage in an experimental autoimmune encephalomyelitis (EAE) mouse model of multiple sclerosis and increased neuronal maturation and survival *in vitro*. A major target of LKE is collapsin response mediator protein 2 (CRMP2), suggesting this protein may mediate LKE actions. We now show that conditional knockout of CRMP2 from neurons using a CamK2a promoter to drive Cre recombinase expression reduces disease severity in the myelin oligodendrocyte glycoprotein $(MOG)_{35–55}$ EAE model, associated with decreased spinal cord axonal damage, and less glial activation in the cerebellum, but not the spinal cord. Immunohistochemical staining and quantitative polymerase chain reaction show CRMP2 depletion from descending motor neurons in the motor cortex, but not from spinal cord neurons, suggesting that the benefits of CRMP2 depletion on EAE may stem from effects on upper motor neurons. In addition, mice in which CRMP2 S522 phosphorylation was prevented by substitution for an alanine residue also showed reduced EAE severity. These results show that modification of CRMP2 expression and phosphorylation can influence the course of EAE and suggests that treatment with CRMP2 modulators such as LKE act in part by reducing CRMP2 S522 phosphorylation.

Keywords

CRMP2, multiple sclerosis, EAE, LKE, spinal cord, upper motor neurons

Received June 20, 2019; Revised October 23, 2019; Accepted for publication November 2, 2019

Introduction

We previously showed that clinical scores in the myelin oligodendrocyte glycoprotein $(MOG)_{35–55}$ peptide-induced experimental autoimmune encephalomyelitis (EAE) model of multiple sclerosis (MS) were significantly reduced by administration of lanthionine ketimine ethyl ester (LKE), accompanied by reductions in axonal damage in spinal cord and optic nerve (Dupree et al., 2015). LKE is a derivatized form of the amino acid lanthionine, a nonproteogenic amino acid synthesized via transulfuration of cysteine with serine by cystathionine-β-synthase (Hensley et al., 2010b). Previous studies showed that LKE promotes growth factor-dependent elongation and thickening of neurites, suppresses TNFα-induced nitric oxide production from microglia, and reduces neurotoxicity due to microglial-conditioned

[1]University of Arizona, Tucson, AZ, USA
[2]University of Illinois, Chicago, IL, USA
[3]Virginia Commonwealth University, Richmond, VA, USA
[4]Universita Cattolica del Sacro Cuore, Rome, Italy
[5]Arkansas College of Osteopathic Medicine, Fort Smith, AR, USA
[6]Jesse Brown VA Medical Center, Chicago, IL, USA

Corresponding Author:
Douglas L. Feinstein, Department of Anesthesiology, 835 South Wolcott Avenue, MC 513, Chicago, IL 60612, USA.
Email: dlfeins@uic.edu

medium (Nada et al., 2012; Hensley et al., 2013). LKE is neuroprotective in mouse models of ischemia (Nada et al., 2012), Alzheimer's disease (AD) (Hensley et al., 2013; Koehler et al., 2018), fluid percussion injury (Hensley et al., 2016), and spinal cord injury (Kotaka et al., 2017). We reported that LKE has direct neuroprotective and neurotrophic effects on human neuroblastoma SH-SY5Y cells and on primary mouse cerebellar granule cells (Marangoni et al., 2018); and that in primary oligodendrocyte progenitor cells (OPCs) LKE induced branch elongation and increased messenger RNA (mRNA) levels of markers of OPC maturation (Savchenko et al., 2019). However, whether the beneficial actions of LKE in EAE are mediated via effects on neurons or other cell types is not yet known.

Despite showing numerous beneficial actions, the mechanisms of action mediating LKE effects remain to be determined. Proteomic studies showed that LKE binds to several proteins present in synaptic complexes, the primary target being collapsin response mediator protein 2 (CRMP2) (Hensley et al., 2010a). CRMP2 is a member of a family of five proteins that act as adaptor proteins and interact with binding partners affecting various cellular functions including division, migration, polarity, synaptic connections, and cytoskeletal architecture (Khanna et al., 2012; Moutal et al., 2019b). In the CNS, CRMP2 has been well characterized with respect to neurite growth and retraction, neural differentiation, axonal transport, and neurotransmitter release (Quach et al., 2004; Chae et al., 2009; Hensley et al., 2011; Quach et al., 2015). CRMP2 and other members of this family are highly expressed in the nervous system during early development, and downregulated in the adult (Quach et al., 2000; Rogemond et al., 2008) where it remains expressed in neurons as well as in glial cells.

CRMP2 effects on axon elongation and neurite extension involve binding to tubulin dimers which are then transferred to the growing plus end of microtubules (Fukata et al., 2002). CRMP2 binding to tubulin is regulated by its phosphorylation status, in particular phosphorylation of serine 522 (S522) by cyclin dependent kinase-5 (Cdk5) (Uchida et al., 2005), which in turn is permissive for phosphorylation at Thr509, 514, and 518 by glycogen synthase kinase 3β (GSK3β) (Uchida et al., 2005). Phosphorylation at these sites reduces CRMP2's affinity for tubulin heterodimers, thus reducing microtubule growth and causing axon retraction (Uchida et al., 2005). Blocking S522A phosphorylation is protective as indicated by findings that the inhibition of Cdk5, or the use of a non-phosphorylatable S522A CRMP2 vector, reduced neurite growth defects in hippocampal cells (Crews et al., 2011); and that knockin (KI) mice with CRMP2 S522A have reduced impairment of synaptic plasticity due to amyloid peptide Aβ (Isono et al., 2013). More recently, interfering with CRMP2 phosphorylation at S522 was shown to reduce pathology in models of Parkinson's disease (PD) (Togashi et al., 2019), chronic pain (Moutal et al., 2016a; Yu et al., 2018; Moutal et al., 2019a), migraine (Moutal et al., 2016b), neurofibromatosis type 1 (NF1) (Moutal et al., 2017b), bipolar disorder (Tobe et al., 2017), glioblastoma (Moutal et al., 2018c), and SOD1G93A amyotrophic lateral sclerosis (ALS) (Numata-Uematsu et al., 2019). It was also reported that CRMP2 phosphorylation plays a critical role in Nogo-receptor signaling (Petratos et al., 2012), and that overexpression of a nonphoshorylatable CRMP2 (at threonine 555) attenuates axonal damage in the optic nerve of EAE mice (Lee et al., 2019). Together these studies point to a role for CRMP2 in modulating disease progression in mouse models of neurodegenerative diseases.

Several studies suggest that LKE works, at least in part, by inhibiting the activity of Cdk5, thus reducing CRMP2 S522A phosphorylation (Hensley et al., 2011; Nada et al., 2012; Hubbard et al., 2013). It is therefore possible that the effects of LKE in $MOG_{35–55}$ peptide induced EAE are mediated by modulation of CRMP2 activity. To begin to address this, we generated CRMP2 conditional knockout (cKO) from neurons and examined the consequences on the development of EAE. We found that the neuronal CRMP2 cKO mice showed reduced clinical signs and less neuropathology as compared to controls. Since CRMP2 phosphorylation regulates its activity, we used the CRMP2-S522A KI mice and found that these mice also show reduced disease severity as compared to wild-type (WT) control mice.

Methods

Mice

All animal studies were approved by both the University of Illinois Chicago and the Jesse Brown VA Institutional Animal Care and Use Committees. Mouse ESCs (Dpysl2tm1a(KOMP)Wtsi, RRID:IMSR_KOMP:CSD38021-1a-Wtsi), harboring a Knockout First, promoter driven CRMP2 allele were obtained from Knockout Mouse Project (KOMP) Repository, rederived, then crossed to Rosa26-FLPe mice (RRID:IMSR_JAX:003946) to delete the neomycin cassette (see Supplemental figure 1) yielding $CRMP2^{f/f}$ mice. $CRMP2^{f/f}$ mice were crossed to CamK2a-CreER(T2) ("Cre," B6;129S6-Tg(Camk2a-cre/ERT2)1Aibs/J, RRID:IMSR_JAX:012362) mice and backcrossed to generate $CRMP2^{f/f}$:$Cre^{+/-}$ and $CRMP2^{f/f}$:$Cre^{-/-}$ mice. Frozen embryos from CRMP2 S522A KI mice (Yamashita et al., 2012) were provided by Dr. Yoshio Goshima (Kanagawa, Japan) and rederived to generate CRMP2 KI and corresponding WT mice (see Supplemental figure 2). Germline transmission was

confirmed by genotyping for the loxP allele in CRMP2$^{f/f}$ mice, and by Sanger sequencing for the A to G substitution in S522A KI mice.

Induction of EAE

Eight-week CRMP2$^{f/f}$:Cre$^{+/-}$ mice were administered tamoxifen (TAM, 100 mg/kg/day, intraperitoneal [i.p.]) for 5 consecutive days to generate CRMP2 cKO mice. CRMP2$^{f/f}$:Cre$^{-/-}$ mice received identical treatment and served as WT controls. EAE reagents were purchased from Hooke Laboratories (EK-2110). In brief, 10-week-old mice (9 days after TAM treatment) were injected with 200 µg of MOG_{35-55} peptide emulsified in CFA (two 100 µl subcutaneous injections into adjacent areas in one hind limb). Two hours later, mice received an i.p. injection of pertussis toxin (PT; 125 ng in 100 µl phosphate-buffered saline [PBS]), then 24 hr later a second PT injection. Clinical signs were scored as follows: 0 = *no clinical signs*, 1 = *limp tail*, 2 = *impaired righting* (unable to return to upright position after placed on back), 3 = *paresis of one hind limb*, 4 = *paresis of two hind limbs*, and 5 = *death*. Scoring was performed every other day at the same time and by the same investigator blinded to allocation. For analysis of variance (ANOVA), if a mouse died or was sacrificed its last score was carried forward till the end of the study.

Immunohistochemistry

Mice were euthanized with carbon dioxide then transcardially perfused with ice-cold PBS. Brains were removed, dissected sagitally at midline, and one hemisphere post-fixed in 4% PFA for 48 hr, followed by 2 days in 30% sucrose for cryoprotection. The other hemisphere was dissected into regions (CB, cerebellum; CTX, cortex) and kept frozen at −80°C till use. Sections (20 µM) were prepared starting at midline. Immunohistochemistry (IHC) was done in cortical areas extending from −1.0 to −2.5 mm relative to Bregma, containing retrosplenial CTX (rCTX); and above the lateral ventricle, extending from 0.5 to 2.0 mm relative to Bregma, which contains motor cortex (mCTX). Spinal cords were removed, and lumbar areas (L1–L4) from four mice processed for IHC and from four mice frozen at −80°C till use. Primary antibodies were rabbit monoclonal anti-CRMP2 (1:1,000, Abcam Cat# ab129082, RRID: AB_11154701), rabbit polyclonal anti-Iba1 (1:1,000, Wako Cat# 019-19741, RRID:AB_839504), rat monoclonal anti-CTIP2 (1:100, Abcam Cat# ab18465, RRID:AB_2064130), and rat monoclonal B2.210 anti-glial fibrillary acidic protein (GFAP, 1:1,000, Thermo Fisher Scientific Cat# 13-0300, RRID:AB_2532994) (Trojanowski et al., 1986). Sections were incubated overnight at 4°C in primary antibody, washed 3 times in PBS for 5 min each, then incubated in rhodamine red- (RRX) or fluorescein- (FITC) conjugated secondary antibodies (1:1,000, Vector Laboratories) in blocking solution. Negative control sections were prepared without primary antibody. Sections were counterstained with DAPI, then mounted with Vectashield® H-1000 mounting medium (Vector Laboratories). Images were collected on a Zeiss Axioplan 2 microscope equipped with an MRm camera using a 40× objective. This provides a field of view of 0.16 mm^2 of which .09 mm^2 is captured by the camera. Axiovision 4.7 software parameters were set to define positive staining versus background values, obtained from the same regions in negative control sections. A cutoff value >10 µm^2 was used to identify cell bodies and processes positively stained for GFAP or Iba1. Staining was quantified in sagittal sections through the cerebellum, with at least four sections per animal and three animals per group, and presented at % area stained.

Immunoblot Analysis

Tissues were homogenized in radioimmunoprecipitation assay (RIPA) buffer (Sigma-Aldrich R0278) containing protease and phosphatase inhibitors (Roche 11836153001). Lysates were cleared by centrifugation and protein concentration measured by bicinchoninic acid (BCA) protein assay (Cat# PI23225, Thermo Fisher Scientific, Waltham, MA). Samples were loaded on 4% to 20% Novex® gels (Cat# EC60285BOX, Thermo Fisher Scientific). Proteins were transferred for 1 hr at 100 V using TGS (25 mM Tris pH = 8.5, 192 mM glycine, 0.1% [mass/vol] sodium dodecyl sulfate), 20% (vol/vol) methanol as transfer buffer to polyvinylidene difluoride (PVDF) membranes 0.45 µm (Cat# IPVH00010, Millipore, Billerica, MA), preactivated in pure methanol. After transfer, membranes were blocked at room temperature for 1 hr with tris-buffered saline with Tween 20 (TBST; 50 mM Tris-HCl, pH 7.4, 150 mM NaCl, 0.1% Tween 20) containing 5% (wt/vol) nonfat dry milk, then incubated separately with the indicated primary antibodies (Table 1) in TBST containing 5% (mass/vol) bovine serum albumin, overnight at 4°C. Following incubation in horseradish peroxidase-conjugated secondary antibodies from Jackson Immunoresearch, blots were revealed by enhanced luminescence (WBKLS0500, Millipore) before exposure to photographic film. Films were scanned, digitized, and quantified using Un-Scan-It gel version 6.1 scanning software by Silk Scientific Inc (Orem, UT). CRMP2 phosphorylation levels were normalized to total CRMP2 levels measured in the same sample, and total CRMP2 levels were normalized to β-actin levels measured in the same sample.

Table 1. Antibodies Used for Immunoblots.

Antibody	Species	Catalog number	Company
CRMP2	Rabbit	C2993, RRID:AB_1078573	Sigma, St. Louis, MO
CRMP2 p32	Rabbit	Generously provided by Dr. Yoshio Goshima (Uchida et al., 2009)	
CRMP2 p509/p514	Sheep	PB-043, RRID:AB_262017	Kinasource, Dundee, Scotland, UK
CRMP2 p522	Rabbit	CP2191, RRID:AB_2094486	ECM Biosciences, Versailles, KY
Actin	Rabbit	A2066, RRID:AB_476693	Sigma, St. Louis, MO

Electron Microscopy Analysis of Axonal Damage

Mice were prepared for transmission electron microscopic analysis as previously described (Dupree and Feinstein, 2018). Mice were transcardially perfused with 0.1 M Millonig's buffer containing 4% paraformaldehyde and 5% glutaraldehyde. Following 2 weeks of aldehyde postfixation, lumbar spinal cords were harvested, rinsed in 0.1M cacodylate buffer, postfixed in 2% osmium tetroxide, rinsed in 0.1 M cacodylate buffer, dehydrated in serial dilutions of ethanol, and embedded in PolyBed 812 resin (PolySciences, Warrington, PA). Ultrathin (70 nm) sections from the lumbar spinal cord levels L2–L3 were stained with uranyl acetate and lead citrate and imaged using a JEOL JEM 1400Plus transmission electron microscope (JEOL, Peabody, MA) equipped with a Gatan OneView CMOS camera (Gatan Inc., Pleasanton, CA). To assess the extent of axonal degeneration, a minimum of 15 electron micrographs (10,000× magnification) were collected per mouse from the lateral columns within 100 μm of the peripheral surface of the cord. These images were used to determine the relative percent of axons undergoing degeneration. Axon degeneration was quantified employing a modification of a classification scheme (Recks et al., 2013) we previously employed (Dupree et al., 2015). Axons were considered damaged if they exhibited one or more of the following: (a) myelin profiles lacking an axon (axolysis, due to either vacuolization or condensation), (b) axonal profiles with an electron dense cytoplasm resulting from dense packing of the cytoskeleton (increased neurofilament density), (c) swollen axons lacking preserved organelles and neurofilaments, (d) axons with swollen mitochondria or mitochondria with disrupted cristae, and (e) axons with obvious loss of contact to myelin.

RNA Isolation

RNA was isolated from whole cerebellum, hippocampus, lumbar spinal cord, and from cerebral cortex from −4 to +3 mm relative to Bregma, which includes visual, somatosensory, parietal, retrosplenial, and motor cortex, cingulate and orbital areas, using Direct-zol RNA MicroPrep (Zymo Research, Irvine, CA) according to instructions. RNA quality was determined using a 4200 TapeStation Instrument (Agilent, Santa Clara, CA), and all samples had RNA integrity values above 8.

Quantitative Real-Time PCR

Total RNA (1 μg) was converted to complementary DNA (cDNA) using the High Capacity cDNA Reverse Transcription Kit (ThermoFisher 4368814). The cDNA was amplified with specific primers using FastStart Universal SYBR Green Master mix (Applied Biosystems, 04913914001) in a Corbett RotoGene real time PCR machine (Qiagen). Relative mRNA levels were calculated from threshold take-off cycle number and normalized to values measured for β-actin in the same samples. Primers were as follows:

CRMP1-forward: 5′-CAGCGTGTCAGGATCAGAAG-3′

CRMP1-reverse: 5′-TTGGTGTTTAGAAGGCGAGG-3′

CRMP2-forward: 5′-CTGACCAGGGAATGACATCC-3′

CRMP2 reverse: 5′-TGATCAAAGGCAGCCAATAGG-3′

β-actin-forward: 5′-CCTGAACTACCCCATTGAACA-3′

β-actin-reverse: 5′-CACACGCAGCTCATTGTAGAA-3′

Data Analysis

Data are presented as mean ± standard error of the mean. Pair-wise comparisons (quantitative polymerase chain reaction [qPCR] data; IHC for GFAP and Iba1; axonal damage) were made using Kruskal–Wallis nonparametric analysis. Comparisons of immunoblot data were made using one-way ANOVA with Tukey post hoc tests. Clinical scores were compared using two-way repeated measures ANOVA and Sidak post hoc analysis.

Results

Generation of Neuronal Conditional Knockout of CRMP2

Neuronal CRMP2 knockout (cKO) mice were generated by administering tamoxifen (100 mg/kg per day for 5 days,

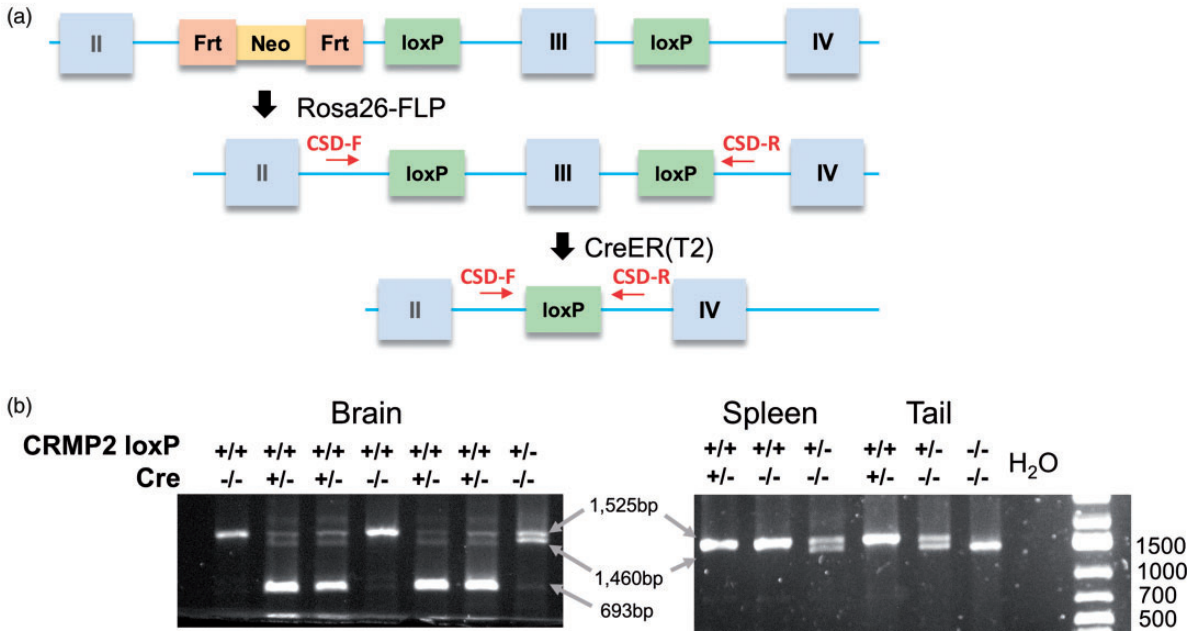

Figure 1. Generation of CRMP2 cKO mice. (a) Schematic showing steps in generation of CRMP2 cKO mice. After removal of the neomycin cassette, the loxP flanked exon III can be removed by Cre recombinase. Full details are provided in Figure S1. (b) PCR of brain, spleen, and tail genomic DNA from tamoxifen-treated CRMP2$^{f/f}$ CamK2aCreER(T2)$^{-/-}$ (WT) and $^{+/-}$ (cKO) mice using primers (shown in red) CSD-F and CSD-R which generate products of 1,460 bp from the WT allele; 1,525 bp from the loxP flanked allele; and 693 bp when exon III is deleted.

i.p.) to 8-week-old CRMP2$^{f/f}$ CamK2aCreER(T2)$^{+/-}$ mice; CRMP2$^{f/f}$ CamK2aCreER(T2) $^{-/-}$ mice treated identically served as WT controls. Two weeks later, exon III deletion was confirmed in the CNS, but not in spleen or tail of Cre$^{+/-}$ cKO mice (Figure 1(a) and (b)). qPCR analysis (Figure 2(a)) showed lower levels of CRMP2 mRNA in CTX, HC, and CB, but not in SC of cKO mice. The partial reductions may be due to CRMP2 expression in CamK2a negative neurons as well as in non-neuronal cells. In contrast, relative levels of CRMP1 mRNA were not significantly reduced in any of the cKO samples, although there were modest, but nonsignificant increases observed in CTX and HC. Immunostaining for CRMP2 showed less staining of granule neurons in the dentate gyrus of the HC (Figure 2(b)), slightly less staining of deep cerebellar neurons in the white matter of the CB (Figure 2(c)) but no changes in staining of SC neurons (Figure 2(d)). Less CRMP2 staining was observed in neurons in the retrosplenial cortex (Figure 2(e)) and the motor cortex (Figure 2(f)). Costaining for Ctip2 (COUP-TF interacting protein 2, a marker of upper motor neurons (Arlotta et al., 2005) showed that CRMP2 was depleted from descending motor neurons (Figure 2(g)).

CRMP2 cKO Reduces EAE Disease Severity

Two weeks after tamoxifen treatment, WT and cKO mice were immunized with MOG_{35-55} peptide. Disease incidence was not affected by genotype and reached 100% in both male and female mice (Figure 3(a) and (c)). In females, average disease onset was not affected by genotype (15.8 ± 1.0 vs. 14.1 ± 1.5 days; WT, cKO); while in males, onset was slightly but not significantly delayed in the cKO mice (13.6 ± 1.2 vs. 15.8 ± 1.5 days; WT, cKO). In female WT mice (Figure 3(b)), disease severity increased between Days 10 and 20 after which there was a slight reduction (however, it was not significant when WT data were analyzed by one-way ANOVA). Disease severity was significantly reduced in cKO mice (two-way ANOVA), which increased after Day 15 but more gradually than in WT mice. In contrast to females, disease severity in male mice was similar in WT and cKO groups (Figure 3(d)). Since only the female cKO mice showed reduced disease severity, further studies were done using samples from female mice.

Assessment of neuroinflammation done at the end of the study (Figure 4(a)) shows that both astrocyte (Figure 4(b)) and microglial (Figure 4(c)) activation was reduced in the cerebellum of cKO mice compared to WT mice, a site of significant glial activation in EAE (Smith and Eng, 1987; Carter et al., 2007; Qin et al., 2012; Gentile et al., 2018; Rossetti et al., 2018). However, in the spinal cord (Figure 4(c)), where significant inflammation and demyelination occurs in this EAE model (Lassmann and Bradl, 2017), the extent of GFAP and Iba1 staining was similar in WT and cKO mice, with

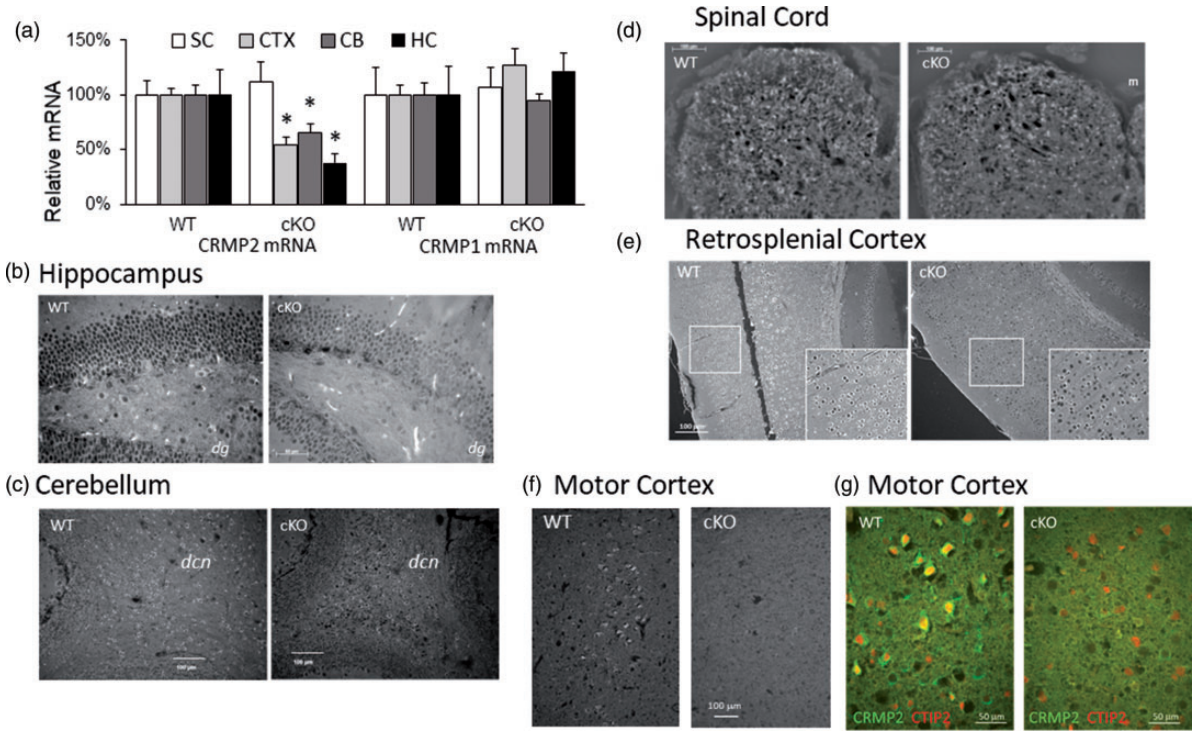

Figure 2. Confirmation of CRMP2 reduction in cKO mice. (a) qPCR for CRMP2 and CRMP1 mRNAs in spinal cord (SC), cortex (CTX), cerebellum (CB), and hippocampus (HC) of WT and cKO mice 2 weeks after treatment with tamoxifen. Data are mean ± *SE*, $n = 4$ per group, normalized to β-actin measured in the same samples, and values for the WT samples set to 100%. *$p < .05$ versus corresponding WT sample. Representative images of immunohistochemical staining of WT and cKO CRMP2 mice for CRMP2 in (b) HC, (c) CB, (d) SC, (e) retrosplenial CTX, and (f) motor CTX. Scale bars are indicated, and the boxed region in panel E is enlarged to show loss of CRMP2 labeled neurons in the subcortical layer. (g) Immunohistochemical staining of motor CTX for CRMP2 (green) and CTIP2 (red) to label descending motor neurons.

a nonsignificant modest increase of Iba1 staining in the cKO mice (Figure 4(d)). Despite the absence of reduced glial cell activation in the spinal cord, EM analysis (Figure 5(a)) revealed a significant reduction in the percentage of damaged axons in the lateral columns of lumbar spinal cord of cKO mice (Figure 5(b)), which are a mix of descending vestibulospinal and corticospinal motor tracts, and descending spinothalamic tracts (Watson and Harrison, 2012). In contrast, there were no differences in plots of g-ratio versus axon caliber (Figure 5(c)) between the WT and cKO EAE mice; nor any differences in average g-ratio, axonal caliber, or myelin thickness (Figure 5(d)).

Effects of CRMP2 cKO on CRMP2 Phosphorylation

The beneficial actions of CRMP2 in several disease models have been ascribed to alterations in its phosphorylation state, since Cdk5-mediated phosphorylation at serine 522 (S522), and subsequent GSK3β phosphorylation at threonine 509 and 514 (T509/514, which requires S522 phosphorylation) inhibits CRMP2 interactions with target proteins including tubulin, calcium channels, and NMDA receptors (Moutal et al., 2019b). To directly test if pS522 plays a role in regulating disease severity, we carried out one study using S522A KI and corresponding congenic WT mice (Yamashita et al., 2007) in which phosphorylation at S522 is prevented. EAE was induced in 10-week-old female KI and WT female mice and disease monitored for 4 weeks (Figure 6). Disease incidence reached 100% in the WT mice and 88% in the KI mice (Figure 6(a)), and the average day of disease onset was similar (13.1 ± 0.5 days vs. 12.3 ± 0.3 days; WT, KI). In the WT group, disease severity increased to Day 16 reaching an average score of 2.7 ± 0.4, after which it did not significantly change reaching 3.0 ± 0.5 at the end of the study (Figure 6(b)). In contrast, while the initial development of disease severity in KI mice was similar to that of the WT mice, reaching an average score of 2.8 ± 0.6 on Day 15, at later times it was significantly less than the WT mice, diminishing to 1.8 ± 0.5 on Day 26, $F(13, 169) = 2.70$, $p = .0018$. Immunoblot analysis of CRMP2 phosphorylation sites (Figure 7(a) and (b)) confirmed that levels of pS522 and pT509/514 were virtually absent from the KI cerebellum (Figure 7(c)) and spinal cords (Figure 7(d)).

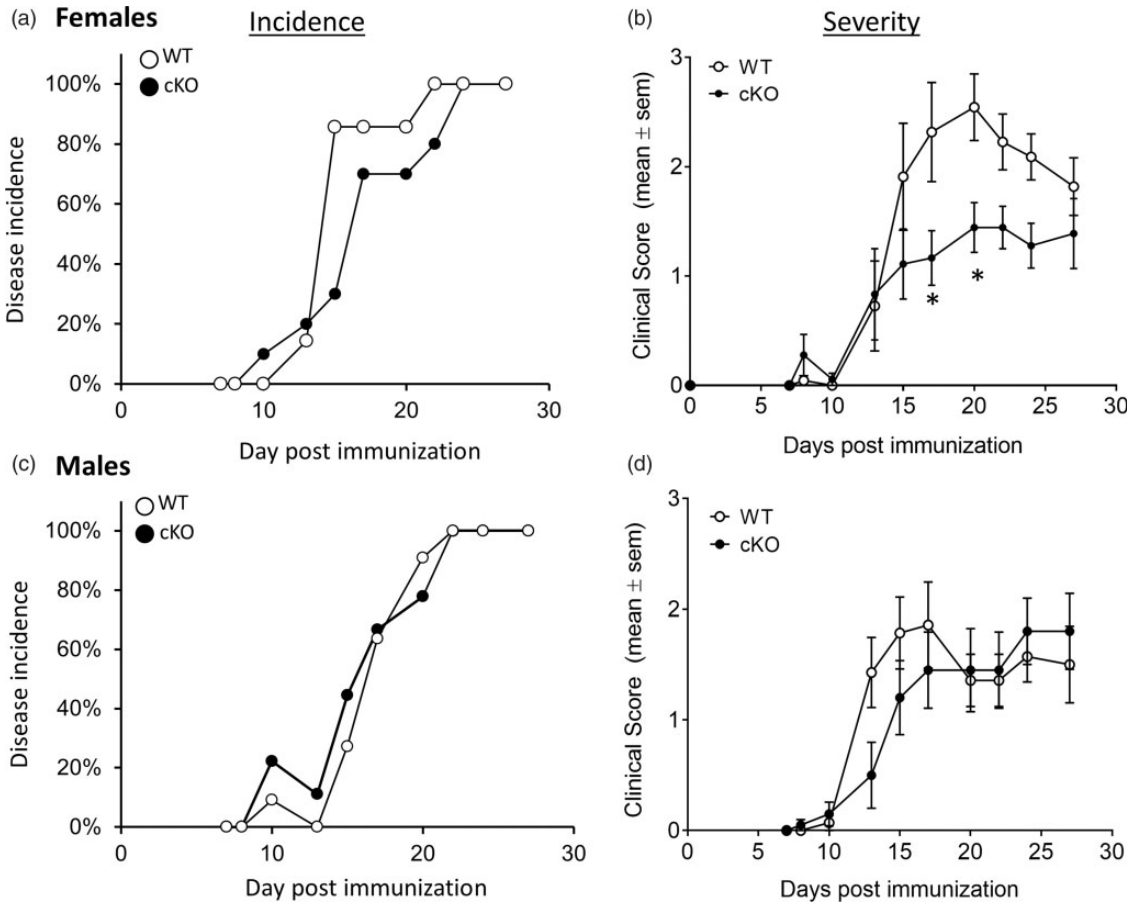

Figure 3. CRMP2 cKO reduces EAE severity. WT and CRMP2 cKO mice were immunized with $MOG_{35–55}$ peptide. Disease incidence reached 100% in both (a) female and (c) male mice and was not affected by genotype. (b) In female mice ($n = 9$ cKO; $n = 11$ WT), disease severity was significantly reduced in the cKO mice (Time × Genotype $F[10, 180) = 2.484$, $p = .0082$, two-way rmANOVA). *$p < .05$ versus WT (Sidak's test). (d) In contrast in male mice, the modest decrease in severity observed at early times did not reach statistical significance—Time × Genotype, $F(10, 150) = 1.442$, $p = .167$. Data are combined from two independent studies. WT = wild-type; cKO = conditional knockout.

Discussion

We previously showed that treatment with the CRMP2 modulator LKE reduced disease severity and axonal damage (Dupree et al., 2015) in MOG peptide induced EAE. Among other proteins, LKE can bind to CRMP2 (Hensley et al., 2010a). This suggests that beneficial actions of LKE in EAE may be mediated, at least in part, to increases in CRMP2 activity. Our findings that LKE exerts direct neuroprotective and neurotrophic effects (Marangoni et al., 2018) prompted us to develop a neuronal CRMP2 cKO mice to explore the roles of neuronal CRMP2 during EAE. In female mice with homozygous neuronal CRMP2 cKO, disease severity was reduced, while in males, although initial disease progression was slightly delayed, it eventually reached similar severity in WT and cKO mice.

Few studies have examined the consequences of CRMP2 depletion from brain. Global knockout of CRMP2 led to cognitive and behavioral deficits in adult mice, suggesting a role for CRMP2 in neuropsychiatric disorders (Nakamura et al., 2016). Brain-specific conditional knockdown of CRMP2 using nestin-Cre mice to drive deletion during early neural development also led to deficits in neuronal development and behavioral impairment in the adults (Zhang et al., 2016). Both global knockout and conditional brain cKO mice showed dysregulation and disorganization of dendritic spine development and patterning (Makihara et al., 2016), which could account for subsequent behavioral deficits. In our studies, CRMP2 deletion was initiated by treatment with tamoxifen at age 8 weeks, 2 weeks prior to induction of EAE. Although we did not yet examine those mice for changes in dendritic complexity or behavior deficits, it is possible that such changes occurred during the short time period and contributed to our findings. However, to our knowledge, the current results represent the first report examining the role of CRMP2 in a model of a neurodegenerative disorder.

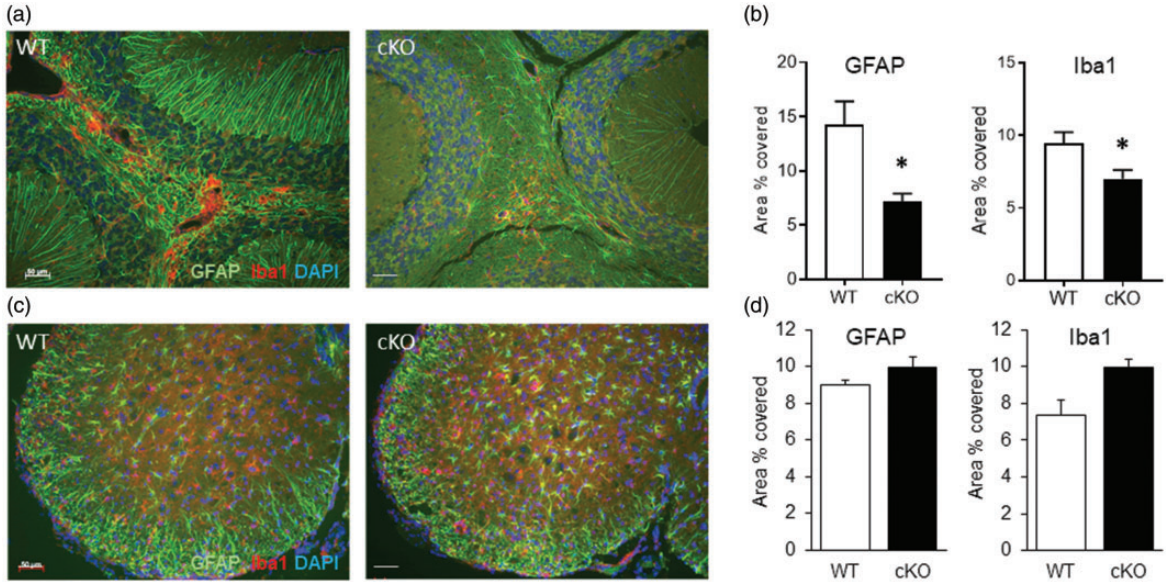

Figure 4. CRMP2 cKO reduces glial activation. Representative images of sagittal sections through (a) the cerebellum and (c) spinal cords of WT and cKO mice, sacrificed at the end of the study shown in Figure 3. At that time, the average EAE scores were 1.4 ($n = 4$, male cKO), 2.5 ($n = 3$, male WT), 1.3 ($n = 3$, female cKO), and 2.2 ($n = 3$, female WT). Sections were stained for GFAP (green) and Iba1 (red), and counter stained with DAPI (blue). The % area stained for GFAP and Iba1 was significantly reduced in the cerebellum (b) but not in the spinal cord (d). Data are mean ± *SE*. *$p < .05$. WT = wild-type; cKO = conditional knockout; GFAP = glial fibrillary acidic protein.

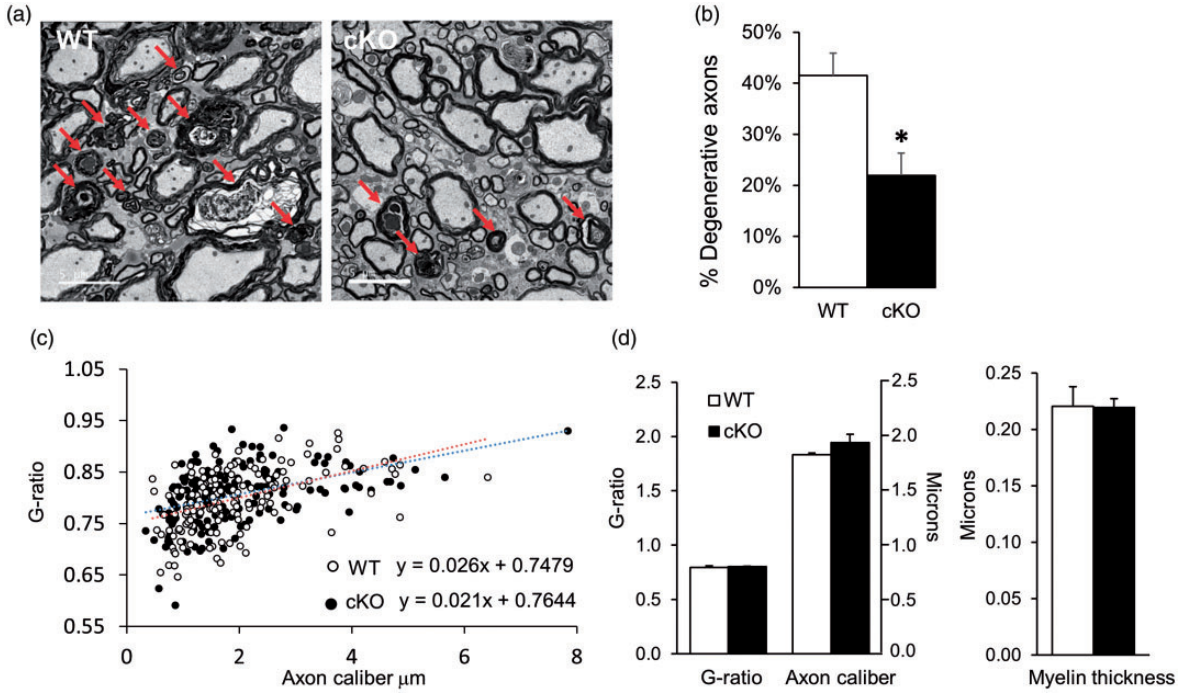

Figure 5. CRMP2 cKO reduces axonal damage without effect on myelin. Spinal cords from WT and cKO EAE female mice were isolated at Day 35 after immunization at which time the average scores were 2.2 ($n = 3$, cKO) and 2.8 ($n = 3$, WT) and processed for electron microscopy. (a) Representative sections of WT and cKO spinal cords. Red arrows indicate damaged axons. (b) Quantitation of the number of damaged axons shows a significant reduction in cKO versus WT mice. Data are mean ± *SE*, $n = 3$ mice per group; and with an average of 700 axons counted in each mouse.*$p < .05$. (c) G-ratios were calculated from measurements of myelin thickness and axon caliber. The linear regression values for WT and cKO groups are shown and were similar in the two groups. (d) Average g-ratio, axonal caliber, and myelin thickness for WT and cKO EAE mice. Values were determined by counting 50 axons from each of three mice per group for a total of 150 axons per group. Data are mean ± *SE*. WT = wild-type; cKO = conditional knockout.

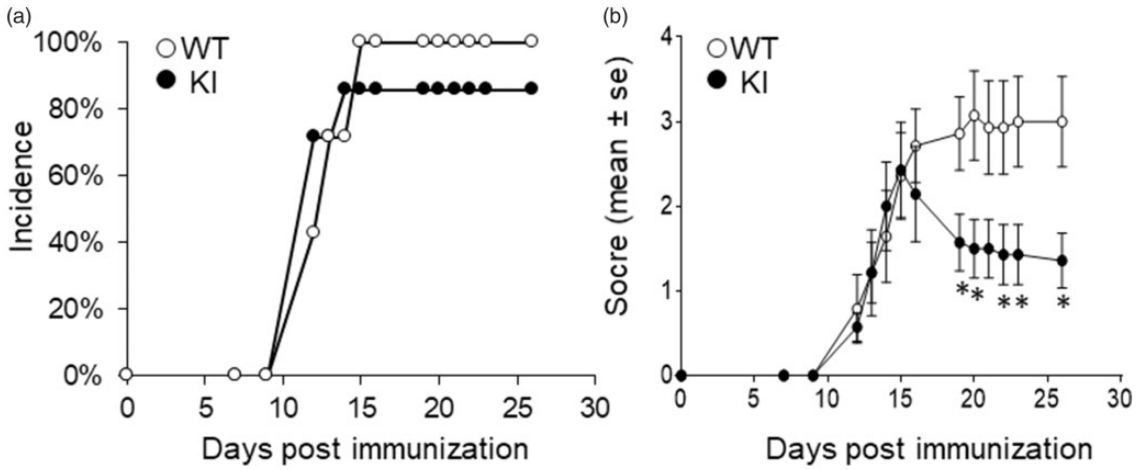

Figure 6. EAE severity is reduced in CRMP2 S522A KI mice. (a) CRMP2 S522A KI and congenic WT female mice were immunized with $MOG_{35–55}$ peptide. Disease incidence reached 100% in the WT (7/7) group and 88% (7/8) in the KI group. (b) Disease severity was significantly lower in the KI compared to WT group—$F(13, 169) = 2.70$, $p = .0018$, two-way repeated measures ANOVA. WT = wild-type; KI = knockin.

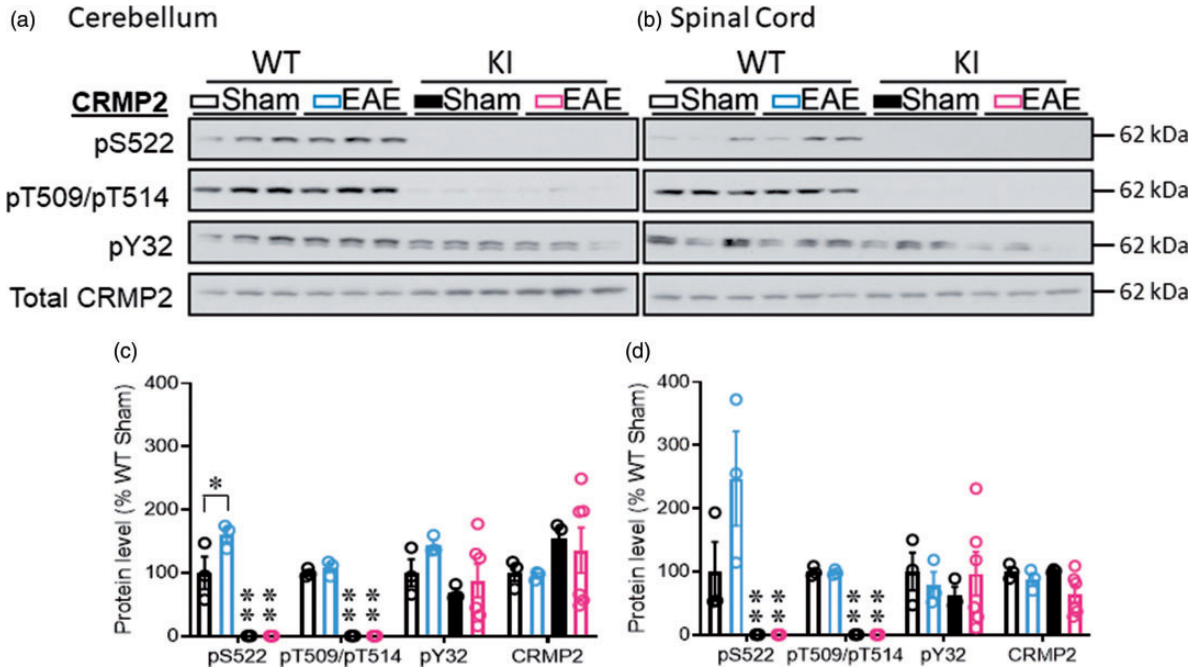

Figure 7. Effects of S522A KI on CRMP2 phosphorylation. Samples from cerebellum and spinal cords of WT and KI, sham and EAE female mice prepared at Day 27 after immunization were used for immunoblot analysis of indicated CRMP2 phosphorylation sites. Representative blots showing three samples per group for (a) cerebellum and (b) spinal cords. Quantitation of indicated CRMP2 phosphorylation sites relative to total CRMP2 levels in (c) cerebellar and (d) spinal cord samples. Data are mean ± *SE*, $n = 3$ (WT Sham), $n = 3$ (WT EAE, average score was 2.2), $n = 3$ (KI Sham), and $n = 5$ (KI EAE, average score was 1.5) samples obtained from 2 EAE studies and show relative levels compared to WT sham. Total CRMP2 levels were normalized to β-actin measured in the same samples. Data are mean ± *SE* and show relative levels compared to WT sham. *$p < .05$, one-way ANOVA, Tukey's test. WT = wild-type; KI = knockin; EAE = experimental autoimmune encephalomyelitis.

IHC staining and qPCR measurements using tissues from naïve (nonimmunized mice) done 2 weeks after treatment with tamoxifen show that CRMP2 expression was reduced, but not eliminated in the HC, CB, and CTX, but not the SC of the cKO mice. Similarly, IHC showed less staining of neurons in the dentate gyrus of the HC, in the white matter of the CB, and in the retrosplenial CTX which lies above the HC. IHC showed

strong depletion of CRMP2 from neurons in the motor cortex which were identified as descending motor neurons by staining for CTIP1, a transcription factor selectively expressed in corticospinal motor neurons and a subset of spinal motor neurons (Yasvoina et al., 2013). In contrast, IHC carried out in sections from the lumbar SC did not reveal any obvious reductions in CRMP2 staining. Although these analyses were not quantified, the combination of qPCR and IHC findings is consistent with CamK2a expression which is high in CTX, HC, and CB but low in SC (Kolker et al., 2012; Gamazon et al., 2018). The partial reductions may also be due, in part, to CRMP2 expression in other cell populations including astrocytes and oligodendrocytes, as well as in non-CamK2a expressing neurons. In addition, since the efficacy of cre-recombinase is typically less than 100%, CRMP2 levels may be reduced, but not absent, in CamK2a expressing neurons.

In this study, EM analysis evaluated ultrastructural alterations in the lateral columns of lumbar spinal cord levels L2 and L3. These columns contain descending spinothalamic (sensory), vestibulospinal (motor), and corticospinal (motor) tracts (Watson and Harrison, 2012). As expected, we observed extensive axonal damage in the WT EAE mice with approximately 40% of counted axons having one or more indices of damage, as compared to a basal level of axonal damage (about 3%) present in sham-immunized mice (Dupree et al., 2015). In cKO mice, axonal damage was reduced to about half of that seen in the WT mice, suggesting that CRMP2 contributes to EAE-induced axonal pathology. Despite the reduction of axonal damage, IHC staining for GFAP and Iba1 did not reveal any reduction of glial activation in the lumbar spinal cord of cKO mice, suggesting that effects on neuroinflammation within the spinal cord did not account for reduced axonal damage. Consistent with this, measurements of axonal caliber and myelin thickness did not show any differences between the WT and the cKO EAE mice. Since $MOG_{35–55}$ peptide EAE largely models a chronic inflammatory encephalopathy (Lassmann and Bradl, 2017), these data suggest that neuronal CRMP2 cKO provides benefit to neurons without affecting inflammatory-induced demyelination in the spinal cord.

Evaluation of CRMP2 expression by qPCR and IHC staining did not show any reduction in the spinal cords of cKO mice; this may be due to lower levels of CamK2a expression in spinal cord neurons (Kolker et al., 2012; Gamazon et al., 2018). In contrast, qPCR of whole cortical samples showed less CRMP2 mRNA in the cKO mice, and IHC identified fewer CRMP2 stained neurons in the motor cortex. These observations suggest that reduced degeneration of spinal cord axons in CRMP2-cKO mice might be associated with protection of corticospinal motor neurons. Mechanistically, the beneficial effect of CRMP2 deletion on EAE-induced degeneration of spinal cord axons may result from preservation of the axon initial segment (AIS), an axonal domain responsible for initiation of the action potential (Buffington and Rasband, 2011). It has been shown that disruption of AIS integrity (number and average length) occurs in EAE mice, associated with increased microglial activation and Ca^{2+} entry (Clark et al., 2016, 2017). Increased Ca^{2+} can activate a variety of proteases including calcineurin and calpain-I which have been shown to cause AIS disruption (Schafer et al., 2009; Benusa et al., 2017). Since CRMP2 interactions with NMDARs and CaV2.2 channels modulate calcium influx into neurons, lower CRMP2 levels in descending motor neurons could lead to reduced Ca^{2+} influx, reduced protease activation, and maintenance of AIS and fiber integrity.

In this study, we also examined the importance of CRMP2 phosphorylation on the development of EAE. pCRMP levels are higher in brains of AD patients compared to controls (Cole et al., 2007; Soutar et al., 2009; Williamson et al., 2011; Hensley and Kursula, 2016), increased in patients with Lewy body dementia (Xing et al., 2016), and are increased after spinal cord injury (Nagai et al., 2016). In neurons, pCRMP2 expression increased due to excitotoxicity (Hou et al., 2009), and in rats, pCRMP2 levels increased in response to intracerebroventricular administration of LPS or TLR4 agonists, and following induction of focal ischemia (Li et al., 2018). We focused attention on CRMP2 phosphorylation occurring at serine 522, a site where reducing or preventing phosphorylation has been shown to mediate neuroprotection and induce axon repair in a number of models of disease and injury. Inhibition of Cdk5, or use of a nonphosphorylatable S522A CRMP2 vector, reduced neurite growth defects in hippocampal cells (Crews et al., 2011); CRMP2 S522A KI mice have reduced impairment of synaptic plasticity due to Aβ (Isono et al., 2013), show delayed Wallerian degeneration (Kinoshita et al., 2019) and increased axonal regeneration (Kondo et al., 2019) due to optic nerve injury; have reduced axonal degradation of dopaminergic neurons in an MPTP model of Parkinson' disease (Togashi et al., 2019); and have delayed motor neuron damage in a transgenic mouse model of ALS (Numata-Uematsu et al., 2019). We found that in CRMP2 S522A KI mice, while disease progression was similar until Day 15 in the KI mice as in their WT controls, after that time disease severity continued to gradually increase in the WT mice while in the KI mice severity significantly lessened. These results suggest that the S522A KI does not affect initial events in the development of EAE which involve T cell activation and migration into the CNS, but instead influences later events such as activation of innate immune responses in parenchymal tissue or neuronal damage. Interestingly, a proteomic analysis comparing

CRMP2 S522A to WT mice showed increases in several proteins, including oligodendrocyte proteins MAG, MOG, and PLP (Nakamura et al., 2018). Since CRMP2 is expressed in adult OLGs and OPC (Dawson et al., 2003; Piaton et al., 2011; Syed et al., 2011; Fernandez-Gamba et al., 2012; Syed et al., 2017), it is possible that in the S522A mice effects in OLGs or OPCs also contributes to reduced EAE severity.

Other phosphorylation sites on CRMP2 also have important roles in regulating axonal damage and regeneration. In particular, CRMP2 phosphorylation at threonine 555 (T555) plays an important role in regulating the extent of axonal damage mediated via signaling through the Nogo receptor (ngr1). In mice with deletion of ngr1, EAE severity was lessened and was associated with preservation of axonal health and myelin integrity (Petratos et al., 2012). In the optic nerve, axonal transport was impaired in the ngr1 null mice, as were interactions of CRMP2 with the axonal motor protein kinesin-1 (Lee et al., 2019), which are increased upon CRMP2 phosphorylation. Moreover, overexpression of a nonphosphorylatable CRMP2T55A also reduced optic nerve axonal degeneration (Lee et al., 2019), showing a critical role for CRMP2 T555 in mediating axonal damage during EAE. In this study, although we ran immunoblots to measure pT555, we were not able to detect this epitope in either spinal cord or cerebellar samples; it remains to be determined if pT555 levels are altered in the optic nerves of CRMP2 cKO EAE mice. We also assessed phosphorylation at CRMP2-Y32, which is increased upregulated following spared nerve injury (Moutal et al., 2019a), and regulates growth cone collapse (Uchida et al., 2009); however, we did not see any change in pY32 in either the CRMP2 cKO mice or the CRMP2 KI mice, suggesting this site may have limited roles during EAE.

CRMP2 roles in axonal guidance were first demonstrated by screening for proteins involved in the collapsin pathway, mediated by Semaphorins (Goshima et al., 1995), and which showed that in response to Semaphorin 3A, CRMP2 induces collapse of the axonal growth cone. CRMP2 was then shown to induce axon elongation and neurite extension, involving binding to tubulin dimers which are transferred to the growing plus end of microtubules (Fukata et al., 2002), as demonstrated by findings that during nerve regeneration, CRMP2 overexpression accelerates axon regeneration and neurite extension (Suzuki et al., 2003). CRMP2 binding to tubulin, as well as to other proteins, is regulated by phosphorylation at Serine 522 by cyclin dependent kinase-5 Cdk5 (Uchida et al., 2005; Moutal et al., 2019b), which in turn is permissive for phosphorylation at Thr509, 514, and 518 by GSK3β (Cole et al., 2004). Phosphorylation at these sites reduces CRMP2's affinity for tubulin heterodimers, thus reducing microtubule growth and causing axon retraction. In addition to tubulin, CRMP2 also interacts with CaV2.2, the presynaptic N-type voltage gated calcium channel (VGCC) (Khanna et al., 2007; Brittain et al., 2009; Moutal et al., 2016c, Moutal et al., 2018b), which regulates neuronal excitability and has roles in neuropathic pain (Francois-Moutal et al., 2015; Xie et al., 2016; Moutal et al., 2017a; Chew and Khanna, 2018; Francois-Moutal et al., 2018; Moutal et al., 2018a). CRMP2 targets CaV2.2 to neuronal membranes (Brittain et al., 2009; Brittain et al., 2011b) and enhances CaV2.2 currents required for transmitter release (Chi et al., 2009). In MS, the α1B subunit of CaV2.2 accumulated in damaged axons in areas of actively demyelinating lesions, suggesting that Ca^{2+} influx contributes to axonal damage (Kornek et al., 2001). Increased α1B expression was also observed in demyelinated axons in a rat model of optic neuritis, and treatment with ω-conotoxin (a selective inhibitor of CaV2.2) reduced axon and myelin damage (Gadjanski et al., 2009). In MOG-peptide EAE, α1B null mice had reduced clinical signs and less demyelination (Tokuhara et al., 2010), and ziconotide (selective CaV2.2 blocker) reduced clinical signs and neuroinflammation (Silva et al., 2018). Together, these findings suggest that reducing CRMP2 could lead to reductions in Ca influx and lessen axonal damage. CRMP2 also interacts with GluN2B containing NMDA receptors (Bretin et al., 2006; Moutal et al., 2014), and disruption of those interactions using CRMP2 derived peptides reduced NMDA-R mediated currents providing neuroprotection against excitotoxicity in animal models of ischemia and traumatic brain injury (Brittain et al., 2011a, 2012; Brustovetsky et al., 2014). These mechanisms that could contribute to the beneficial effects in CRMP2 cKO mice are summarized in Figure 8.

In summary, our findings demonstrate that CRMP2 deficiency from neurons can reduce the severity of disease in the $MOG_{35–55}$ peptide induced EAE model of MS, which was associated with decreases in axonal damage in spinal cord tracts. These effects may be mediated, at least in part, by reduced CRMP2 in upper motor neurons, whose fibers traverse through the cerebellum and comprise descending cortico-spinal tracts. Evaluation of glial activation revealed a reduction of astrocyte and microglial activation in the cerebellum of cKO mice, but not in the spinal cord. Neuroinflammation in $MOG_{35–55}$ peptide induced EAE in mice primarily occurs in white matter tracks of the cerebellum, brainstem, and in the optic nerves (Lassmann and Bradl, 2017), which contrasts to what occurs in MS patients where neuroinflammation is observed in subcortical areas. It therefore will be important to extend the current findings to other CNS regions and other models of MS disease. Our findings using S522A KI mice show that disease severity is also reduced in the absence of

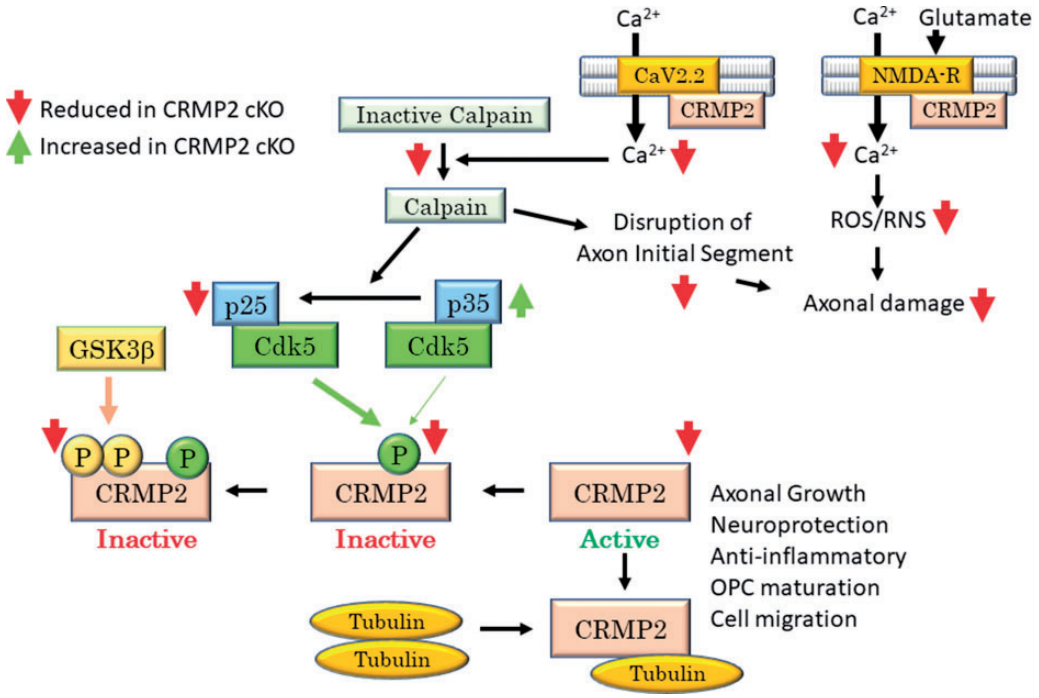

Figure 8. Possible mechanisms underlying reduced neuropathology in CRMP2 cKO mice. In cKO mice, CRMP2 remaining in CamK2a expressing neurons, and CRMP2 expressed in other cells, shows reduced phosphorylation at both S522 and T509/514. Reduced phosphorylation at S522 could be due to reduced Cdk5 activity, as suggested by results showing an increase in the relative levels of the Cdk5 modulator p35 to p25 (although increases in selective phosphatases could also play a role). Conversion of p35 to p35 is mediated by calpain-1, which is converted from an inactive to active form requiring intracellular Ca^{2+}. Lower CRMP2 levels will reduce Ca^{2+} influx through the N-type voltage gated calcium channel (CaV2.2), thereby reducing calpain-1 activation. CRMP2 regulation of the NMDA-receptors (NMDA-R) will also be reduced in cKO cells, leading to lower glutamate dependent Ca^{2+} influx, formation of reactive oxygen and nitrogen species, and reduced neurotoxicity. These events may be occurring in descending motor neurons, thereby reducing damage to the axon initial segment whose disruption can contribute to axonal damage.

CRMP2 phosphorylation at serine 522, consistent with other studies showing reduced pathology in these mice; however, additional studies are needed to determine if glial activation or axonal damage is also lessened in the KI mice. Together our results demonstrate that modulating CRMP2 expression or phosphorylation state can provide benefit in EAE and suggest that actions on CRMP2 mediate, at least in part, the effects of LKE observed during EAE.

Acknowledgments

The authors thank Dr. Gerardo Morfini for providing CTIP2 antibody and helpful discussion. CRMP2 S522A mice were provided by Dr. Yoshio Goshima.

Declaration of Conflicting Interests

The author(s) declared no potential conflicts of interest with respect to the research, authorship, and/or publication of this article.

Funding

The author(s) disclosed receipt of the following financial support for the research, authorship, and/or publication of this article: This work was supported by grant RG-1501-02654 from the National Multiple Sclerosis Society (D. L. F.); grant 14S-RCS-003 from the Department of Veterans Affairs (D. L. F.); and NIH grants 1R01NS098772 and 1R01DA042852 (R. K.).

ORCID iDs

Rajesh Khanna https://orcid.org/0000-0002-9066-2969
Douglas L. Feinstein https://orcid.org/0000-0003-2815-2885

Supplemental Material

Supplemental material for this article is available online.

References

Arlotta, P., Molyneaux, B. J., Chen, J., Inoue, J., Kominami, R., & Macklis, J. D. (2005). Neuronal subtype-specific genes that control corticospinal motor neuron development in vivo. *Neuron*, *45*, 207–221.

Benusa, S. D., George, N. M., Sword, B. A., DeVries, G. H., & Dupree, J. L. (2017). Acute neuroinflammation induces AIS structural plasticity in a NOX2-dependent manner. *J Neuroinflammation*, *14*, 116.

Bretin, S., Rogemond, V., Marin, P., Maus, M., Torrens, Y., Honnorat, J., Glowinski, J., Premont, J., & Gauchy, C. (2006). Calpain product of WT-CRMP2 reduces the amount of surface NR2B NMDA receptor subunit. *J Neurochem*, *98*, 1252–1265.

Brittain, J. M., Chen, L., Wilson, S. M., Brustovetsky, T., Gao, X., Ashpole, N. M., Molosh, A. I., You, H., Hudmon, A., Shekhar, A., White, F. A., Zamponi, G. W., Brustovetsky, N., Chen, J., & Khanna, R. (2011a). Neuroprotection against traumatic brain injury by a peptide derived from the collapsin response mediator protein 2 (CRMP2). *J Biol Chem*, *286*, 37778–37792.

Brittain, J. M., et al. (2011b). Suppression of inflammatory and neuropathic pain by uncoupling CRMP-2 from the presynaptic ca(2)(+) channel complex. *Nat Med*, *17*, 822–829.

Brittain, J. M., Pan, R., You, H., Brustovetsky, T., Brustovetsky, N., Zamponi, G. W., Lee, W. H., & Khanna, R. (2012). Disruption of NMDAR-CRMP-2 signaling protects against focal cerebral ischemic damage in the rat middle cerebral artery occlusion model. *Channels (Austin)*, *6*, 52–59.

Brittain, J. M., Piekarz, A. D., Wang, Y., Kondo, T., Cummins, T. R., & Khanna, R. (2009). An atypical role for collapsin response mediator protein 2 (CRMP-2) in neurotransmitter release via interaction with presynaptic voltage-gated calcium channels. *J Biol Chem*, *284*, 31375–31390.

Brustovetsky, T., Pellman, J. J., Yang, X. F., Khanna, R., & Brustovetsky, N. (2014). Collapsin response mediator protein 2 (CRMP2) interacts with n-methyl-d-aspartate (NMDA) receptor and na+/ca2+ exchanger and regulates their functional activity. *J Biol Chem*, *289*, 7470–7482.

Buffington, S. A., & Rasband, M. N. (2011). The axon initial segment in nervous system disease and injury. *Eur J Neurosci*, *34*, 1609–1619.

Carter, S. L., Muller, M., Manders, P. M., & Campbell, I. L. (2007). Induction of the genes for Cxcl9 and Cxcl10 is dependent on IFN-gamma but shows differential cellular expression in experimental autoimmune encephalomyelitis and by astrocytes and microglia in vitro. *Glia*, *55*, 1728–1739.

Chae, Y. C., Lee, S., Heo, K., Ha, S. H., Jung, Y., Kim, J. H., Ihara, Y., Suh, P. G., & Ryu, S. H. (2009). Collapsin response mediator protein-2 regulates neurite formation by modulating tubulin GTPase activity. *Cell Signal*, *21*, 1818–1826.

Chew, L. A., & Khanna, R. (2018). CRMP2 and voltage-gated ion channels: Potential roles in neuropathic pain. *Neuronal Signal*, *2*, NS20170220.

Chi, X. X., Schmutzler, B. S., Brittain, J. M., Wang, Y., Hingtgen, C. M., Nicol, G. D., & Khanna, R. (2009). Regulation of n-type voltage-gated calcium channels (Cav2.2) and transmitter release by collapsin response mediator protein-2 (CRMP-2) in sensory neurons. *J Cell Sci*, *122*, 4351–4362.

Clark, K. C., Josephson, A., Benusa, S. D., Hartley, R. K., Baer, M., Thummala, S., Joslyn, M., Sword, B. A., Elford, H., Oh, U., Dilsizoglu-Senol, A., Lubetzki, C., Davenne, M., DeVries, G. H., & Dupree, J. L. (2016). Compromised axon initial segment integrity in EAE is preceded by microglial reactivity and contact. *Glia*, *64*, 1190–1209.

Clark, K. C., Sword, B. A., & Dupree, J. L. (2017). Oxidative stress induces disruption of the axon initial segment. *ASN Neuro*, *9*, 1759091417745426.

Cole, A. R., Knebel, A., Morrice, N. A., Robertson, L. A., Irving, A. J., Connolly, C. N., & Sutherland, C. (2004). Gsk-3 phosphorylation of the Alzheimer epitope within collapsin response mediator proteins regulates axon elongation in primary neurons. *J Biol Chem*, *279*, 50176–50180.

Cole, A. R., Noble, W., van Aalten, L., Plattner, F., Meimaridou, R., Hogan, D., Taylor, M., LaFrancois, J., Gunn-Moore, F., Verkhratsky, A., Oddo, S., LaFerla, F., Giese, K. P., Dineley, K. T., Duff, K., Richardson, J. C., Yan, S. D., Hanger, D. P., Allan, S. M., & Sutherland, C. (2007). Collapsin response mediator protein-2 hyperphosphorylation is an early event in Alzheimer's disease progression. *J Neurochem*, *103*, 1132–1144.

Crews, L., Ruf, R., Patrick, C., Dumaop, W., Trejo-Morales, M., Achim, C. L., Rockenstein, E., & Masliah, E. (2011). Phosphorylation of collapsin response mediator protein-2 disrupts neuronal maturation in a model of adult neurogenesis: Implications for neurodegenerative disorders. *Mol Neurodegener*, *6*, 67.

Dawson, J., Hotchin, N., Lax, S., & Rumsby, M. (2003). Lysophosphatidic acid induces process retraction in CG-4 line oligodendrocytes and oligodendrocyte precursor cells but not in differentiated oligodendrocytes. *J Neurochem*, *87*, 947–957.

Dupree, J. L., & Feinstein, D. L. (2018). Influence of diet on axonal damage in the EAE mouse model of multiple sclerosis. *J Neuroimmunol*, *322*, 9–14.

Dupree, J. L., Polak, P. E., Hensley, K., Pelligrino, D., & Feinstein, D. L. (2015). Lanthionine ketimine ester provides benefit in a mouse model of multiple sclerosis. *J Neurochem*, *134*, 302–314.

Fernandez-Gamba, A., Leal, M. C., Maarouf, C. L., Richter-Landsberg, C., Wu, T., Morelli, L., Roher, A. E., & Castano, E. M. (2012). Collapsin response mediator protein-2 phosphorylation promotes the reversible retraction of oligodendrocyte processes in response to non-lethal oxidative stress. *J Neurochem*, *121*, 985–995.

Francois-Moutal, L., Dustrude, E. T., Wang, Y., Brustovetsky, T., Dorame, A., Ju, W., Moutal, A., Perez-Miller, S., Brustovetsky, N., Gokhale, V., Khanna, M., & Khanna, R. (2018). Inhibition of the Ubc9 E2 sumo-conjugating enzyme-CRMP2 interaction decreases NaV1.7 currents and reverses experimental neuropathic pain. *Pain*, *159*, 2115–2127.

Francois-Moutal, L., Wang, Y., Moutal, A., Cottier, K. E., Melemedjian, O. K., Yang, X., Wang, Y., Ju, W., Largent-Milnes, T. M., Khanna, M., Vanderah, T. W., & Khanna, R. (2015). A membrane-delimited n-myristoylated CRMP2 peptide aptamer inhibits Cav2.2 trafficking and reverses inflammatory and postoperative pain behaviors. *Pain*, *156*, 1247–1264.

Fukata, Y., Itoh, T. J., Kimura, T., Menager, C., Nishimura, T., Shiromizu, T., Watanabe, H., Inagaki, N., Iwamatsu, A., Hotani, H., & Kaibuchi, K. (2002). CRMP-2 binds to tubulin heterodimers to promote microtubule assembly. *Nat Cell Biol*, *4*, 583–591.

Gadjanski, I., Boretius, S., Williams, S. K., Lingor, P., Knoferle, J., Sattler, M. B., Fairless, R., Hochmeister, S., Suhs, K. W., Michaelis, T., Frahm, J., Storch, M. K., Bahr M, & Diem R (2009). Role of n-type voltage-dependent calcium channels in autoimmune optic neuritis. *Ann Neurol*, *66*, 81–93.

Gamazon, E. R., Segre, A. V., van de Bunt, M., Wen, X., Xi, H. S., Hormozdiari, F., Ongen, H., Konkashbaev, A., Derks, E. M., Aguet, F., Quan, J., Nicolae, D. L., Eskin, E., Kellis, M., Getz, G., McCarthy, M. I., Dermitzakis, E. T., Cox, N. J., & Ardlie, K. G. (2018). Using an atlas of gene regulation across 44 human tissues to inform complex disease- and trait-associated variation. *Nat Genet*, *50*, 956–967.

Gentile, A., Musella, A., De Vito, F., Fresegna, D., Bullitta, S., Rizzo, F. R., Centonze, D., & Mandolesi, G. (2018). Laquinimod ameliorates excitotoxic damage by regulating glutamate re-uptake. *J Neuroinflammation*, *15*, 5.

Goshima, Y., Nakamura, F., Strittmatter, P., & Strittmatter, S. M. (1995). Collapsin-induced growth cone collapse mediated by an intracellular protein related to UNC-33. *Nature*, *376*, 509–514.

Hensley, K., Christov, A., Kamat, S., Zhang, X. C., Jackson, K. W., Snow, S., & Post, J. (2010a). Proteomic identification of binding partners for the brain metabolite lanthionine ketimine (LK) and documentation of LK effects on microglia and motoneuron cell cultures. *J Neurosci*, *30*, 2979–2988.

Hensley, K., Gabbita, S. P., Venkova, K., Hristov, A., Johnson, M. F., Eslami, P., & Harris-White, M. E. (2013). A derivative of the brain metabolite lanthionine ketimine improves cognition and diminishes pathology in the 3 x Tg-AD mouse model of Alzheimer disease. *J Neuropathol Exp Neurol*, *72*, 955–969.

Hensley, K., & Kursula, P. (2016). Collapsin response mediator protein-2 (CRMP2) is a plausible etiological factor and potential therapeutic target in Alzheimer's disease: Comparison and contrast with microtubule-associated protein tau. *J Alzheimers Dis*, *53*, 1–14.

Hensley, K., Poteshkina, A., Johnson, M. F., Eslami, P., Gabbita, S. P., Hristov, A. M., Venkova-Hristova, K. M., & Harris-White, M. E. (2016). Autophagy modulation by lanthionine ketimine ethyl ester improves long-term outcome after central fluid percussion injury in the mouse. *J Neurotrauma*, *33*, 1501–1513.

Hensley, K., Venkova, K., & Christov, A. (2010b) Emerging biological importance of central nervous system lanthionines. *Molecules*, *15*, 5581–5594.

Hensley, K., Venkova, K., Christov, A., Gunning, W., & Park, J. (2011). Collapsin response mediator protein-2: An emerging pathologic feature and therapeutic target for neurodisease indications. *Mol Neurobiol*, *43*, 180–191.

Hou, S. T., Jiang, S. X., Aylsworth, A., Ferguson, G., Slinn, J., Hu, H., Leung, T., Kappler, J., & Kaibuchi, K. (2009). Camkii phosphorylates collapsin response mediator protein 2 and modulates axonal damage during glutamate excitotoxicity. *J Neurochem*, *111*, 870–881.

Hubbard, C., Benda, E., Hardin, T., Baxter, T., St, J. E., O'Brien, S., Hensley, K., & Holgado, A. M. (2013). Lanthionine ketimine ethyl ester partially rescues neurodevelopmental defects in UNC-33 (DPYSL2/CRMP2) mutants. *J Neurosci Res*, *91*, 1183–1190.

Isono, T., Yamashita, N., Obara, M., Araki, T., Nakamura, F., Kamiya, Y., Alkam, T., Nitta, A., Nabeshima, T., Mikoshiba, K., Ohshima, T., & Goshima, Y. (2013). Amyloid-beta(2)(5)(-)(3)(5) induces impairment of cognitive function and long-term potentiation through phosphorylation of collapsin response mediator protein 2. *Neurosci Res*, *77*, 180–185.

Khanna, R., Wilson, S. M., Brittain, J. M., Weimer, J., Sultana, R., Butterfield, A., & Hensley, K. (2012). Opening Pandora's jar: A primer on the putative roles of CRMP2 in a panoply of neurodegenerative, sensory and motor neuron, and central disorders. *Future Neurol*, *7*, 749–771.

Khanna, R., Zougman, A., & Stanley, E. F. (2007). A proteomic screen for presynaptic terminal n-type calcium channel (Cav2.2) binding partners. *J Biochem Mol Biol*, *40*, 302–314.

Kinoshita, Y., Kondo, S., Takahashi, K., Nagai, J., Wakatsuki, S., Araki, T., Goshima, Y., & Ohshima, T. (2019). Genetic inhibition of CRMP2 phosphorylation delays Wallerian degeneration after optic nerve injury. *Biochem Biophys Res Commun*, *514*, 1037–1039.

Koehler, D., Shah, Z. A., Hensley, K., & Williams, F. E. (2018). Lanthionine ketimine-5-ethyl ester provides neuroprotection in a zebrafish model of okadaic acid-induced Alzheimer's disease. *Neurochem Int*, *115*, 61–68.

Kolker, E., Higdon, R., Haynes, W., Welch, D., Broomall, W., Lancet, D., Stanberry, L., & Kolker, N. (2012). Moped: Model organism protein expression database. *Nucleic Acids Res*, *40*, D1093–1099.

Kondo, S., Takahashi, K., Kinoshita, Y., Nagai, J., Wakatsuki, S., Araki, T., Goshima, Y., & Ohshima, T. (2019). Genetic inhibition of CRMP2 phosphorylation at serine 522 promotes axonal regeneration after optic nerve injury. *Sci Rep*, *9*, 7188.

Kornek, B., Storch, M. K., Bauer, J., Djamshidian, A., Weissert, R., Wallstroem, E., Stefferl, A., Zimprich, F., Olsson, T., Linington, C., Schmidbauer, M., & Lassmann, H. (2001). Distribution of a calcium channel subunit in dystrophic axons in multiple sclerosis and experimental autoimmune encephalomyelitis. *Brain*, *124*, 1114–1124.

Kotaka, K., Nagai, J., Hensley, K., & Ohshima, T. (2017). Lanthionine ketimine ester promotes locomotor recovery after spinal cord injury by reducing neuroinflammation and promoting axon growth. *Biochem Biophys Res Commun*, *483*, 759–764.

Lassmann, H., & Bradl, M. (2017). Multiple sclerosis: Experimental models and reality. *Acta Neuropathol*, *133*, 223–244.

Lee, J. Y., Kim, M. J., Thomas, S., Oorschot, V., Ramm, G., Mun Aui, P., Sekine, Y., Deliyanti, D., Wilkinson-Berka, J., Niego, B., Harvey, A. R., Theotokis, P., McLean, C., Strittmatter, S. M., & Petratos, S. (2019). Limiting neuronal Nogo receptor 1 signaling during experimental autoimmune

encephalomyelitis (EAE) preserves axonal transport and abrogates inflammatory demyelination. *J Neurosci*, *39*, 5562–5580.

Li, X. B., Ding, M. X., Ding, C. L., Li, L. L., Feng, J., & Yu, X. J. (2018). Toll-like receptor 4 promotes the phosphorylation of CRMP2 via the activation of Rhokinase in MCAO rats. *Mol Med Rep*, *18*, 342–348.

Makihara, H., Nakai, S., Ohkubo, W., Yamashita, N., Nakamura, F., Kiyonari, H., Shioi, G., Jitsuki-Takahashi, A., Nakamura, H., Tanaka, F., Akase, T., Kolattukudy, P., & Goshima, Y. (2016). CRMP1 and CRMP2 have synergistic but distinct roles in dendritic development. *Genes Cells*, *21*, 994–1005.

Marangoni, N., Kowal, K., Deliu, Z., Hensley, K., & Feinstein, D. L. (2018). Neuroprotective and neurotrophic effects of lanthionine ketimine ester. *Neurosci Lett*, *664*, 28–33.

Moutal, A., Chew, L. A., Yang, X., Wang, Y., Yeon, S. K., Telemi, E., Meroueh, S., Park, K. D., Shrinivasan, R., Gilbraith, K. B., Qu, C., Xie, J. Y., Patwardhan, A., Vanderah, T. W., Khanna, M., Porreca, F., & Khanna, R. (2016a). (S)-lacosamide inhibition of CRMP2 phosphorylation reduces postoperative and neuropathic pain behaviors through distinct classes of sensory neurons identified by constellation pharmacology. *Pain*, *157*, 1448–1463.

Moutal, A., Dustrude, E. T., Largent-Milnes, T. M., Vanderah, T. W., Khanna, M., & Khanna, R. (2018a). Blocking CRMP2 sumoylation reverses neuropathic pain. *Mol Psychiatry*, *23*, 2119–2121.

Moutal, A., Eyde, N., Telemi, E., Park, K. D., Xie, J. Y., Dodick, D. W., Porreca, F., & Khanna, R. (2016b). Efficacy of (s)-lacosamide in preclinical models of cephalic pain. *Pain Rep*, *1*. doi: 10.1097/PR9.0000000000000565

Moutal, A., Francois-Moutal, L., Brittain, J. M., Khanna, M., & Khanna, R. (2014). Differential neuroprotective potential of CRMP2 peptide aptamers conjugated to cationic, hydrophobic, and amphipathic cell penetrating peptides. *Front Cell Neurosci*, *8*, 471.

Moutal, A., Francois-Moutal, L., Perez-Miller, S., Cottier, K., Chew, L. A., Yeon, S. K., Dai, J., Park, K. D., Khanna, M., & Khanna, R. (2016c). (S)-lacosamide binding to collapsin response mediator protein 2 (CRMP2) regulates cav2.2 activity by subverting its phosphorylation by cdk5. *Mol Neurobiol*, *53*, 1959–1976.

Moutal, A., Li, W., Wang, Y., Ju, W., Luo, S., Cai, S., Francois-Moutal, L., Perez-Miller, S., Hu, J., Dustrude, E. T., Vanderah, T. W., Gokhale, V., Khanna, M., & Khanna, R. (2018b). Homology-guided mutational analysis reveals the functional requirements for antinociceptive specificity of collapsin response mediator protein 2-derived peptides. *Br J Pharmacol*, *175*, 2244–2260.

Moutal, A., Luo, S., Largent-Milnes, T. M., Vanderah, T. W., & Khanna, R. (2019a). Cdk5-mediated CRMP2 phosphorylation is necessary and sufficient for peripheral neuropathic pain. *Neurobiol Pain*, *5*, 100022.

Moutal, A., Sun, L., Yang, X., Li, W., Cai, S., Luo, S., & Khanna, R. (2018c). CRMP2-neurofibromin interface drives NF1-related pain. *Neuroscience*, *381*, 79–90.

Moutal, A., Wang, Y., Yang, X., Ji, Y., Luo, S., Dorame, A., Bellampalli, S. S., Chew, L. A., Cai, S., Dustrude, E. T., Keener, J. E., Marty, M. T., Vanderah, T. W., & Khanna, R. (2017a). Dissecting the role of the CRMP2-neurofibromin complex on pain behaviors. *Pain*, *158*, 2203–2221.

Moutal, A., White, K. A., Chefdeville, A., Laufmann, R. N., Vitiello, P. F., Feinstein, D., Weimer, J. M., & Khanna, R. (2019b). Dysregulation of CRMP2 post-translational modifications drive its pathological functions. *Mol Neurobiol*, *56*, 6736–6755.

Moutal, A., Yang, X., Li, W., Gilbraith, K. B., Luo, S., Cai, S., Francois-Moutal, L., Chew, L. A., Yeon, S. K., Bellampalli, S. S., Qu, C., Xie, J. Y., Ibrahim, M. M., Khanna, M., Park, K. D., Porreca, F., & Khanna, R. (2017b). CRISPR/Cas9 editing of nf1 gene identifies CRMP2 as a therapeutic target in neurofibromatosis type 1-related pain that is reversed by (s)-lacosamide. *Pain*, *158*, 2301–2319.

Nada, S. E., Tulsulkar, J., Raghavan, A., Hensley, K., & Shah, Z. A. (2012). A derivative of the CRMP2 binding compound lanthionine ketimine provides neuroprotection in a mouse model of cerebral ischemia. *Neurochem Int*, *61*, 1357–1363.

Nagai, J., Owada, K., Kitamura, Y., Goshima, Y., & Ohshima, T. (2016). Inhibition of CRMP2 phosphorylation repairs CNS by regulating neurotrophic and inhibitory responses. *Exp Neurol*, *277*, 283–295.

Nakamura, H., Takahashi-Jitsuki, A., Makihara, H., Asano, T., Kimura, Y., Nakabayashi, J., Yamashita, N., Kawamoto, Y., Nakamura, F., Ohshima, T., Hirano, H., Tanaka, F., & Goshima, Y. (2018). Proteome and behavioral alterations in phosphorylation-deficient mutant collapsin response mediator protein2 knock-in mice. *Neurochem Int*, *119*, 207–217.

Nakamura, H., Yamashita, N., Kimura, A., Kimura, Y., Hirano, H., Makihara, H., Kawamoto, Y., Jitsuki-Takahashi, A., Yonezaki, K., Takase, K., Miyazaki, T., Nakamura, F., Tanaka, F., & Goshima, Y. (2016). Comprehensive behavioral study and proteomic analyses of CRMP2-deficient mice. *Genes Cells*, *21*, 1059–1079.

Numata-Uematsu, Y., Wakatsuki, S., Nagano, S., Shibata, M., Sakai, K., Ichinohe, N., Mikoshiba, K., Ohshima, T., Yamashita, N., Goshima, Y., & Araki, T. (2019). Inhibition of collapsin response mediator protein-2 phosphorylation ameliorates motor phenotype of ALS model mice expressing SOD1G93A. *Neurosci Res*, *139*, 63–68.

Petratos, S., Ozturk, E., Azari, M. F., Kenny, R., Lee, J. Y., Magee, K. A., Harvey, A. R., McDonald, C., Taghian, K., Moussa, L., Mun, A. P., Siatskas, C., Litwak, S., Fehlings, M. G., Strittmatter, S. M., & Bernard, C. C. (2012). Limiting multiple sclerosis related axonopathy by blocking Nogo receptor and CRMP-2 phosphorylation. *Brain*, *135*, 1794–1818.

Piaton, G., Aigrot, M. S., Williams, A., Moyon, S., Tepavcevic, V., Moutkine, I., Gras, J., Matho, K. S., Schmitt, A., Soellner, H., Huber, A. B., Ravassard, P., & Lubetzki, C. (2011). Class 3 semaphorins influence oligodendrocyte precursor recruitment and remyelination in adult central nervous system. *Brain*, *134*, 1156–1167.

Qin, H., Yeh, W. I., De Sarno, P., Holdbrooks, A. T., Liu, Y., Muldowney, M. T., Reynolds, S. L., Yanagisawa, L. L., Fox, T. H., 3rd, Park, K., Harrington, L. E., Raman, C.,

& Benveniste, E. N. (2012). Signal transducer and activator of transcription-3/suppressor of cytokine signaling-3 (STAT3/SOCS3) axis in myeloid cells regulates neuroinflammation. *Proc Natl Acad Sci U S A*, *109*, 5004–5009.

Quach, T. T., Duchemin, A. M., Rogemond, V., Aguera, M., Honnorat, J., Belin, M. F., & Kolattukudy, P. E. (2004). Involvement of collapsin response mediator proteins in the neurite extension induced by neurotrophins in dorsal root ganglion neurons. *Mol Cell Neurosci*, *25*, 433–443.

Quach, T. T., Honnorat, J., Kolattukudy, P. E., Khanna, R., & Duchemin, A. M. (2015). CRMPs: Critical molecules for neurite morphogenesis and neuropsychiatric diseases. *Mol Psychiatry*, *20*, 1037–1045.

Quach, T. T., Mosinger, B., Jr., Ricard, D., Copeland, N. G., Gilbert, D. J., Jenkins, N. A., Stankoff, B., Honnorat, J., Belin, M. F., & Kolattukudy, P. (2000). Collapsin response mediator protein-3/UNC-33-like protein-4 gene: Organization, chromosomal mapping and expression in the developing mouse brain. *Gene*, *242*, 175–182.

Recks, M. S., Stormanns, E. R., Bader, J., Arnhold, S., Addicks, K., & Kuerten, S. (2013). Early axonal damage and progressive myelin pathology define the kinetics of CNS histopathology in a mouse model of multiple sclerosis. *Clin Immunol*, *149*, 32–45.

Rogemond, V., Auger, C., Giraudon, P., Becchi, M., Auvergnon, N., Belin, M. F., Honnorat, J., & Moradi-Ameli, M. (2008). Processing and nuclear localization of CRMP2 during brain development induce neurite outgrowth inhibition. *J Biol Chem*, *283*, 14751–14761.

Rossetti, I., Zambusi, L., Finardi, A., Bodini, A., Provini, L., Furlan, R., & Morara, S. (2018). Calcitonin gene-related peptide decreases Il-1beta, Il-6 as well as Ym1, Arg1, CD163 expression in a brain tissue context-dependent manner while ameliorating experimental autoimmune encephalomyelitis. *J Neuroimmunol*, *323*, 94–104.

Savchenko, V., Kalinin, S., Boullerne, A. I., Kowal, K., Lin, S. X., & Feinstein, D. L. (2019). Effects of the CRMP2 activator lanthionine ketimine ethyl ester on oligodendrocyte progenitor cells. *J Neuroimmunol*, *334*, 576977.

Schafer, D. P., Jha, S., Liu, F., Akella, T., McCullough, L. D., & Rasband, M. N. (2009). Disruption of the axon initial segment cytoskeleton is a new mechanism for neuronal injury. *J Neurosci*, *29*, 13242–13254.

Silva, R. B. M., Greggio, S., Venturin, G. T., da Costa, J. C., Gomez, M. V., & Campos, M. M. (2018). Beneficial effects of the calcium channel blocker ctk 01512-2 in a mouse model of multiple sclerosis. *Mol Neurobiol*, *55*, 9307–9327.

Smith, M. E., & Eng, L. F. (1987). Glial fibrillary acidic protein in chronic relapsing experimental allergic encephalomyelitis in SJL/J mice. *J Neurosci Res*, *18*, 203–208.

Soutar, M. P., Thornhill, P., Cole, A. R., & Sutherland, C. (2009). Increased CRMP2 phosphorylation is observed in Alzheimer's disease; does this tell us anything about disease development? *Curr Alzheimer Res*, *6*, 269–278.

Suzuki, Y., Nakagomi, S., Namikawa, K., Kiryu-Seo, S., Inagaki, N., Kaibuchi, K., Aizawa, H., Kikuchi, K., & Kiyama, H. (2003). Collapsin response mediator protein-2 accelerates axon regeneration of nerve-injured motor neurons of rat. *J Neurochem*, *86*, 1042–1050.

Syed, Y. A., Abdulla, S. A., & Kotter, M. R. (2017). Studying the effects of semaphorins on oligodendrocyte lineage cells. *Methods Mol Biol*, *1493*, 363–378.

Syed, Y. A., Hand, E., Mobius, W., Zhao, C., Hofer, M., Nave, K. A., & Kotter, M. R. (2011). Inhibition of CNS remyelination by the presence of semaphorin 3a. *J Neurosci*, *31*, 3719–3728.

Tobe, B. T. D., et al. (2017). Probing the lithium-response pathway in hiPSCs implicates the phosphoregulatory set-point for a cytoskeletal modulator in bipolar pathogenesis. *Proc Natl Acad Sci U S A*, *114*, E4462–E4471.

Togashi, K., Hasegawa, M., Nagai, J., Tonouchi, A., Masukawa, D., Hensley, K., Goshima, Y., & Ohshima, T. (2019). Genetic suppression of collapsin response mediator protein 2 phosphorylation improves outcome in methyl-4-phenyl-1,2,3,6-tetrahydropyridine-induced Parkinson's model mice. *Genes Cells*, *24*, 31–40.

Tokuhara, N., Namiki, K., Uesugi, M., Miyamoto, C., Ohgoh, M., Ido, K., Yoshinaga, T., Yamauchi, T., Kuromitsu, J., Kimura, S., Miyamoto, N., & Kasuya, Y. (2010). N-type calcium channel in the pathogenesis of experimental autoimmune encephalomyelitis. *J Biol Chem*, *285*, 33294–33306.

Trojanowski, J. Q., Walkenstein, N., & Lee, V. M. (1986). Expression of neurofilament subunits in neurons of the central and peripheral nervous system: An immunohistochemical study with monoclonal antibodies. *J Neurosci*, *6*, 650–660.

Uchida, Y., Ohshima, T., Sasaki, Y., Suzuki, H., Yanai, S., Yamashita, N., Nakamura, F., Takei, K., Ihara, Y., Mikoshiba, K., Kolattukudy, P., Honnorat, J., & Goshima, Y. (2005). Semaphorin3a signalling is mediated via sequential cdk5 and gsk3beta phosphorylation of CRMP2: Implication of common phosphorylating mechanism underlying axon guidance and Alzheimer's disease. *Genes Cells*, *10*, 165–179.

Uchida, Y., Ohshima, T., Yamashita, N., Ogawara, M., Sasaki, Y., Nakamura, F., & Goshima, Y. (2009). Semaphorin3a signaling mediated by Fyn-dependent tyrosine phosphorylation of collapsin response mediator protein 2 at tyrosine 32. *J Biol Chem*, *284*, 27393–27401.

Watson, C., & Harrison, M. (2012). The location of the major ascending and descending spinal cord tracts in all spinal cord segments in the mouse: Actual and extrapolated. *Anat Rec (Hoboken)*, *295*, 1692–1697.

Williamson, R., van Aalten, L., Mann, D. M., Platt, B., Plattner, F., Bedford, L., Mayer, J., Howlett, D., Usardi, A., Sutherland, C., & Cole, A. R. (2011). CRMP2 hyperphosphorylation is characteristic of Alzheimer's disease and not a feature common to other neurodegenerative diseases. *J Alzheimers Dis*, *27*, 615–625.

Xie, J. Y., Chew, L. A., Yang, X., Wang, Y., Qu, C., Wang, Y., Federici, L. M., Fitz, S. D., Ripsch, M. S., Due, M. R., Moutal, A., Khanna, M., White, F. A., Vanderah, T. W., Johnson, P. L., Porreca, F., & Khanna, R. (2016). Sustained relief of ongoing experimental neuropathic pain by a CRMP2 peptide aptamer with low abuse potential. *Pain*, *157*, 2124–2140.

Xing, H., Lim, Y. A., Chong, J. R., Lee, J. H., Aarsland, D., Ballard, C. G., Francis, P. T., Chen, C. P., & Lai, M. K.

(2016). Increased phosphorylation of collapsin response mediator protein-2 at thr514 correlates with beta-amyloid burden and synaptic deficits in Lewy body dementias. *Mol Brain*, *9*, 84.

Yamashita, N., Morita, A., Uchida, Y., Nakamura, F., Usui, H., Ohshima, T., Taniguchi, M., Honnorat, J., Thomasset, N., Takei, K., Takahashi, T., Kolattukudy, P., & Goshima, Y. (2007). Regulation of spine development by semaphorin3a through cyclin-dependent kinase 5 phosphorylation of collapsin response mediator protein 1. *J Neurosci*, *27*, 12546–12554.

Yamashita, N., Ohshima, T., Nakamura, F., Kolattukudy, P., Honnorat, J., Mikoshiba, K., & Goshima, Y. (2012). Phosphorylation of CRMP2 (collapsin response mediator protein 2) is involved in proper dendritic field organization. *J Neurosci*, *32*, 1360–1365.

Yasvoina, M. V., Genc, B., Jara, J. H., Sheets, P. L., Quinlan, K. A., Milosevic, A., Shepherd, G. M., Heckman, C. J., & Ozdinler, P. H. (2013). eGFP expression under UCHL1 promoter genetically labels corticospinal motor neurons and a subpopulation of degeneration-resistant spinal motor neurons in an ALS mouse model. *J Neurosci*, *33*, 7890–7904.

Yu, J., Moutal, A., Dorame, A., Bellampalli, S. S., Chefdeville, A., Kanazawa, I., Pham, N. Y. N., Park, K. D., Weimer, J. M., & Khanna, R. (2018). Phosphorylated CRMP2 regulates spinal nociceptive neurotransmission. *Mol Neurobiol*, *56*, 5241–5255.

Zhang, H., Kang, E., Wang, Y., Yang, C., Yu, H., Wang, Q., Chen, Z., Zhang, C., Christian, K. M., Song, H., Ming, G. L., & Xu, Z. (2016). Brain-specific CRMP2 deletion leads to neuronal development deficits and behavioural impairments in mice. *Nat Commun*, *7*, 11773.